A Letters Journal Exploring the Frontiers of Physics

September 2022

EPL, **139** (2022) 66001
doi: 10.1209/0295-5075/ac8c69

www.epljournal.org

Probing the response of metals to low-frequency s-polarized evanescent fields

G. L. Klimchitskaya[1,2(a)], V. M. Mostepanenko[1,2,3] and V. B. Svetovoy[4]

[1] *Central Astronomical Observatory at Pulkovo of the Russian Academy of Sciences - Saint Petersburg, 196140, Russia*
[2] *Peter the Great Saint Petersburg Polytechnic University - Saint Petersburg, 195251, Russia*
[3] *Kazan Federal University - Kazan, 420008, Russia*
[4] *Frumkin Institute of Physical Chemistry and Electrochemistry, Russian Academy of Sciences Leninsky prospect 31 bld. 4, 119071 Moscow, Russia*

received 11 July 2022; accepted in final form 24 August 2022
published online 2 September 2022

Abstract – An experimental test for the response function of metals to the low-frequency *s*-polarized evanescent waves is proposed by measuring the lateral component of the magnetic field of an oscillating magnetic dipole spaced above a thick metallic plate. This suggestion is motivated by the fact that the Lifshitz theory using the Drude response function is in contradiction with high-precision measurements of the Casimir force performed at separations exceeding 150 nm. Analytic expressions for the lateral components of the magnetic field, which are fully determined by the *s*-polarized evanescent waves, are reported in terms of the reflection coefficients of the plate metal. Numerical computations are performed for the reasonable values of the experimental parameters for different models of the dielectric response. The resulting fields differ by the orders of magnitude depending on whether the Drude or plasma response function is used in computations. Thus, the measurement of the magnetic field will allow to discriminate between these two options. Possible applications of the obtained results are discussed.

Introduction. – The evanescent fields are created by the oscillating currents and charges, which are always present in a metal interior. It has been known that they are confined in the vicinity of metallic surfaces and are characterized by the zero mean Poynting vector. The respective solution to the wave equation is characterized by at least one pure imaginary component of the wave vector. This leads to the exponentially fast drop of the evanescent wave in the corresponding spatial directions (see the monographs [1,2] for theory and diverse applications of evanescent waves).

In spite of the paramount importance of some applications, *e.g.*, as a tool to overcome the diffraction limit in optics [3], the electromagnetic response of metals to the *s*-polarized evanescent waves is still not sufficiently investigated. A large body of information is collected on surface plasmon polaritons [4] for large magnitudes $k_t = |\boldsymbol{k}_t|$ of the wave vector projection on the surface. This information, however, refers solely to the transverse magnetic (*p*-polarized) evanescent waves. At the same time a much used technique of the total internal reflection and frustrated total internal reflection enables to probe the electromagnetic response of metals in the area of k_t only somewhat over the wave vector magnitude $k_0 = \omega/c$ where ω is the field frequency [5–7]. The reason is that for transparent media the index of refraction in the infrared domain is not sufficiently large (*e.g.*, for Si it is equal to only 3.4). Note also that the method of nano frustrated total internal reflection used in the near-field optical microscopy to overcome the diffraction limit [3,8] is more sensitive to the *p*-polarized evanescent waves [9].

The response of metals to the low-frequency electromagnetic waves (including the evanescent ones) is routinely described by means of the Drude model. Recently, however, the use of this model in the case of *s*-polarized evanescent waves has been questioned by a series of high-precision experiments on measuring the Casimir force between metallic surfaces performed at separations above

(a) E-mail: g.klimchitskaya@gmail.com (corresponding author)

150 nm [10–22]. The point is that the measurement data of these experiments are inconsistent with theoretical predictions of the fundamental Lifshitz theory [23–25] if the electromagnetic response of metals at low frequencies is described by the Drude model. The surprising thing is that the same measurement data were found to be in good agreement with theory if the plasma model is used although this model disregards the relaxation properties of conduction electrons and should not be applicable at low frequencies [10–22]. A more sophisticated treatment of the problem revealed that the major difference between the theoretical predictions for the Casimir force using the Drude and plasma models originates from the contribution of s-polarized low-frequency evanescent waves [26–31] (see also reviews in [32–34]). This places strong emphasis on an independent test of the response function of metals to the s-type evanescent waves.

In this letter, we derive an analytic expression for the magnetic field of an oscillating magnetic dipole spaced in vacuum at some height above a thick metallic plate. The magnetic moment of this dipole is pointed perpendicular to the plate. According to our results obtained in the general case of a spatially nonlocal electromagnetic response, the lateral component of the magnetic field is determined by the s-polarized low-frequency evanescent waves and is highly sensitive to the character of response function of the metal. Based on this, we propose an experimental test for a response function to the s-type evanescent waves. Computations are made for typical experimental parameters. It is shown that the magnitudes of lateral component of the dipole magnetic field computed using the Drude and plasma models differ by up to a factor of several thousands depending on the dipole oscillation frequency. This allows to either confirm or exclude the theoretical description of the response of metals to the s-polarized evanescent waves by means of the Drude model. The possible implication of the suggested test for the Casimir physics and in a wider context for condensed matter physics and optics is discussed.

Magnetic dipole above metallic plate. – First let us consider the oscillating magnetic dipole in vacuum in the absence of metallic plate. We assume that it is at the origin of the coordinates $\boldsymbol{r}_0 = (0,0,0)$ and the magnetic moment $\boldsymbol{m} = [0,0,m_0\exp(-i\omega t)]$ is directed along the z-axis. On the assumption that the dipole size is much smaller than the wavelength $\lambda = 2\pi c/\omega$, the components of its magnetic field at a point $\boldsymbol{r} = (x,y,z) \equiv (x_1,x_2,z)$ are given by [35] (here and below it is implied that all fields depend on t as $\exp(-i\omega t)$)

$$\begin{aligned} H_{x_\alpha}(\omega,\boldsymbol{r}) &= -m_0\frac{x_\alpha z}{r^2}\left(\frac{k_0^2}{r}+3i\frac{k_0}{r^2}-\frac{3}{r^3}\right)e^{ik_0r}, \\ H_z(\omega,\boldsymbol{r}) &= m_0\left[\frac{k_0^2}{r}+i\frac{k_0}{r^2}-\frac{1}{r^3}\right. \\ &\quad \left.-\frac{z^2}{r^2}\left(\frac{k_0^2}{r}+3i\frac{k_0}{r^2}-\frac{3}{r^3}\right)\right]e^{ik_0r}, \end{aligned} \tag{1}$$

where $\alpha = 1,\ 2$, $k_0 \equiv \omega/c$, $r = |\boldsymbol{r}| = (x^2+y^2+z^2)^{1/2}$, and the Gaussian system of units is used.

The components of the electric field of magnetic dipole in free space are [35]

$$\boldsymbol{E}(\omega,\boldsymbol{r}) = im_0k_0\left(i\frac{k_0}{r^2}-\frac{1}{r^3}\right)e^{ik_0r}\begin{pmatrix} y \\ -x \\ 0 \end{pmatrix}. \tag{2}$$

Note that the magnitudes of the electric field components are suppressed by a factor k_0r in comparison with those for the magnetic field. Since in the suggested experimental test $k_0r < 10^{-9}$ (see below), the electric field of the dipole can be ignored.

In what follows we shall use the Fourier expansion of the field (1) in two-dimensional plane waves

$$\boldsymbol{H}(\omega,\boldsymbol{r}) = \frac{1}{(2\pi)^2}\int \mathrm{d}\boldsymbol{k}_t e^{i\boldsymbol{k}_t\boldsymbol{r}_t}\boldsymbol{H}(\omega,\boldsymbol{k}_t,z), \tag{3}$$

where $\boldsymbol{k}_t = (k_x,k_y) \equiv (k_1,k_2)$ and $\boldsymbol{r}_t = (x,y) \equiv (x_1,x_2)$. The explicit expressions for the Fourier transform $\boldsymbol{H}(\omega,\boldsymbol{k}_t,z)$ can be easily found in the polar coordinates using the integral representation for the Bessel functions [36] and several integrals [37,38]. The results are

$$\begin{aligned} H_{x_\alpha}(\omega,\boldsymbol{k}_t,z) &= -2\pi i m_0 k_\alpha \mathrm{sign}(z)e^{-q|z|}, \\ H_z(\omega,\boldsymbol{k}_t,z) &= 2\pi m_0\frac{k_t^2}{q}e^{-q|z|}, \end{aligned} \tag{4}$$

where $k_t^2 = k_x^2+k_y^2$ and $q = (k_t^2-k_0^2)^{1/2}$.

We are coming now to the case of magnetic dipole located at the point $(0,0,h)$ above the surface of a thick metallic plate coinciding with the coordinate plane $z=0$ (see fig. 1). The field of this dipole in the region above the plate can be calculated by the method of images [39,40]. This method reduces to an introduction of the fictitious image source whose field is identical to the field of induced charges on the plate. Originally, it was used to solve the boundary problems for static fields and ideal metal surfaces. However, it is also applicable for the quasistatic fields [41]. We consider this case and assume that the dipole size is much smaller than h which, in its turn, is much smaller than $\lambda = 2\pi c/\omega$. Note that we have reproduced the same results, as obtained below, with the help of a technically more complicated but fully rigorous method of Green functions used in the derivation of the Lifshitz formula for the Casimir force in [23–25]. According to the method of images, the field in question can be found as a superposition of the fields of the real dipole and the fictitious (image) dipole located at the point $(0,0,-h)$. In so doing the magnetic moment of the image dipole depends on the reflectivity properties of metallic plate.

The reflectivity properties are usually described by the Fresnel reflection coefficients defined for p- and s-polarizations of the electromagnetic field

$$R_p(\omega,k_t) = \frac{\varepsilon(\omega)q-q_\varepsilon}{\varepsilon(\omega)q+q_\varepsilon}, \quad R_s(\omega,k_t) = \frac{q-q_\varepsilon}{q+q_\varepsilon}, \tag{5}$$

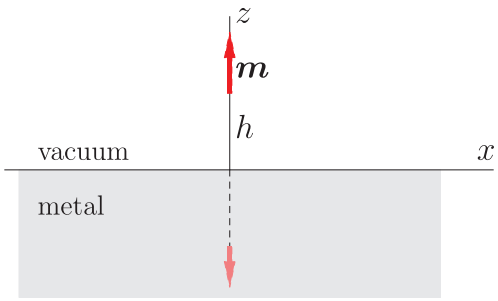

Fig. 1: Configuration of magnetic dipole spaced in vacuum above thick metallic plate and the fictitious (image) dipole.

where $q_\varepsilon = [k_t^2 - \varepsilon(\omega)k_0^2]^{1/2}$ and $\varepsilon(\omega)$ is the frequency-dependent dielectric permittivity of the plate metal. In this section, however, we do not use a specific form of the reflection coefficients making the results applicable to both the local and nonlocal response of the metal (note that the spatially nonlocal models are the subject of considerable discussion in relation to the problems of the Lifshitz theory mentioned above [42–53]). It has to be stressed also that in the configuration of fig. 1 the reflected wave is determined by the coefficient R_s alone because the electric field remains negligibly small.

Now we apply eq. (4) to both the dipole and its image in order to find the Fourier transform of the magnetic field above the surface of metallic plate. After taking into account that in the coordinate system of fig. 1 one has to replace z with $z-(-h)=z+h$ for the fictitious dipole and with $z-h$ for the real one, the result is

$$\begin{aligned} H_{x_\alpha}^{(p)}(\omega,\boldsymbol{k}_t,z) &= -2\pi i m_0 k_\alpha \left[R_s(\omega,k_t)e^{-q(z+h)} \right. \\ &\quad \left. +\mathrm{sign}(z-h)e^{-q|z-h|}\right], \\ H_z^{(p)}(\omega,\boldsymbol{k}_t,z) &= 2\pi m_0 \frac{k_t^2}{q}[R_s(\omega,k_t)e^{-q(z+h)} \\ &\quad +e^{-q|z-h|}]. \end{aligned} \tag{6}$$

Substituting eq. (6) into eq. (3) and using eq. (1) for the second terms on the right-hand side of eq. (6), we find the magnetic field in the domain above the metallic plate,

$$\begin{aligned} H_{x_\alpha}^{(p)}(\omega,\boldsymbol{r}) &= -\frac{im_0}{2\pi}\int \mathrm{d}\boldsymbol{k}_t R_s(\omega,k_t)k_\alpha e^{i\boldsymbol{k}_t\boldsymbol{r}_t-q(z+h)} \\ &\quad -m_0\frac{x_\alpha(z-h)}{r^2}\left(\frac{k_0^2}{r}+3i\frac{k_0}{r^2}-\frac{3}{r^3}\right)e^{ik_0r}, \\ H_z^{(p)}(\omega,\boldsymbol{r}) &= \frac{m_0}{2\pi}\int \mathrm{d}\boldsymbol{k}_t R_s(\omega,k_t)\frac{k_t^2}{q}e^{i\boldsymbol{k}_t\boldsymbol{r}_t-q(z+h)} \\ &\quad +m_0\left[\frac{k_0^2}{r}+i\frac{k_0}{r^2}-\frac{1}{r^3}\right. \\ &\quad \left.-\frac{(z-h)^2}{r^2}\left(\frac{k_0^2}{r}+3i\frac{k_0}{r^2}-\frac{3}{r^3}\right)\right]e^{ik_0r}, \end{aligned} \tag{7}$$

where now $r=[x^2+y^2+(z-h)^2]^{1/2}$.

Introducing the polar coordinates under the integrals on the right-hand sides in eq. (7) and integrating over the angle variable [36,37], one arrives at

$$\begin{aligned} H_{x_\alpha}^{(p)}(\omega,\boldsymbol{r}) &= \frac{m_0x_\alpha}{r_t}\int_0^\infty \mathrm{d}k_t k_t^2 J_1(k_tr_t)R_s(\omega,k_t)e^{-q(z+h)} \\ &\quad -m_0\frac{x_\alpha(z-h)}{r^2}\left(\frac{k_0^2}{r}+3i\frac{k_0}{r^2}-\frac{3}{r^3}\right)e^{ik_0r}, \\ H_z^{(p)}(\omega,\boldsymbol{r}) &= m_0\int_0^\infty \mathrm{d}k_t\frac{k_t^3}{q}J_0(k_tr_t)R_s(\omega,k_t)e^{-q(z+h)} \\ &\quad +m_0\left[\frac{k_0^2}{r}+i\frac{k_0}{r^2}-\frac{1}{r^3}\right. \\ &\quad \left.-\frac{(z-h)^2}{r^2}\left(\frac{k_0^2}{r}+3i\frac{k_0}{r^2}-\frac{3}{r^3}\right)\right]e^{ik_0r}, \end{aligned} \tag{8}$$

where J_n is the Bessel function and $r_t=(x_1^2+x_2^2)^{1/2}$ is the polar radial variable.

In the strict sense, both the propagating waves (for them $k_t<k_0$ and q is pure imaginary) and the evanescent waves (for them $k_t>k_0$ and q is real) contribute to the field (8). For the propagating waves, however, the power in the exponential factors under the integral is pure imaginary: $-q(z+h)=i(k_0^2-k_t^2)^{1/2}(z+h)$. Since in the suggested experimental test $k_0r\ll 1$ holds or, equivalently, $r\ll\lambda$, it is possible to neglect by the phase in these factors. As a result, one can see that the contribution of propagating waves to the integrals in eq. (8) is less than that of the evanescent ones by the factor of $1/(k_0h)^3=\lambda^3/(2\pi h)^3$. Below we choose $h\sim r$ in the suggested experimental test leading to $1/(k_0h)^3\sim 10^{27}$. Because of this one can neglect the contribution of propagating waves and replace the lower integration limits in eq. (8) with k_0.

Another important observation is that the contribution of the real dipole to the total magnetic field above the plate (8) vanishes for the lateral components $H_{x_\alpha}^{(p)}$ and becomes simpler for the z-component $H_z^{(p)}$ if the calculation is performed at the dipole height $z=h$. Since we are looking for a quantity which is the most sensitive to the response function of metal to the evanescent waves, there are no better candidates than the lateral components of the magnetic field given by

$$H_{x_\alpha}^{(p)}(\omega,\boldsymbol{r})=\frac{m_0x_\alpha}{r_t}\int_{k_0}^\infty \mathrm{d}k_t k_t^2 J_1(k_tr_t)R_s(\omega,k_t)e^{-2qh}. \tag{9}$$

In fact eq. (9) is analogous to the Lifshitz formula for the Casimir force at large separations. In this case, the difference in Casimir forces calculated using the Drude and plasma dielectric functions is completely determined by different contributions of the s-polarized evanescent waves. Thus, calculating the field components (9) for different models of the dielectric response of metal and comparing the obtained results with the measurement data, taken at $z=h$, it is possible to independently test the validity of these models in the range of low-frequency evanescent waves.

Parameters of magnetic dipole. – The magnetic dipole considered in the previous section can be realized in the form of an alternating current $I_0 \exp(-i\omega t)$ which flows through a small circular loop of radius R or a coil containing N loops. In such a situation, the magnitude of the magnetic moment is given by

$$m_0 = \frac{1}{c}\pi N I_0 R^2. \tag{10}$$

It is assumed that the coil size is much smaller than the height h above the plate where it is situated (see fig. 1).

The qualitative assessment for the desirable parameters of the coil can be made under a simplified assumption of an ideal metal plate, *i.e.*, by putting $R_s(\omega, k_t) = -1$. In this case from eq. (6) we obtain the Fourier transform of the x-component of magnetic field calculated at height $z = h$ above the plate,

$$H_x^{(p)}(\omega, \boldsymbol{k}_t, h) = 2\pi i m_0 k_x e^{-2hq}. \tag{11}$$

By comparing this with eq. (4), one can conclude that under a condition $k_0 r \ll 1$ the x-component of magnetic field is given by the last term on the right-hand side of eq. (1) with $z = 2h$,

$$H_x^{(p)}(x) = \frac{6m_0 x h}{(x^2+4h^2)^{5/2}} = \frac{m_0}{h^3}\frac{6\tilde{x}}{(4+\tilde{x}^2)^{5/2}}, \tag{12}$$

where we introduced the dimensionless variable $\tilde{x} = x/h$.

From (12) it is seen that in order to maximize the lateral projection of magnetic field one should have larger m_0 (*i.e.*, higher current and larger loop radius and the number of loops) but smaller distance between the dipole and the plate.

It is rather difficult to create the magnetic dipole which combines a high electric current with small h because the coil size is supposed to be much smaller than h. Fabrication of a small coil with a high current and large number of loops presents a real challenge. Micro electromagnets which meet our requirements have been, however, created using the methods of micro [54–56] and mini [39] technologies. The typical micro electromagnet may be of 1 mm height and consist of $N = 10$ loops of $R = 1$ mm radius. The coil of this kind is able to support the current up to $I_0 = 3 \times 10^9$ stat A which is equal to 1 A in the SI. Calculating the respective magnetic moment by (10), one finds

$$m_0 = 3.14 \times 10^{-2}\,\text{erg/Oe} = 3.14 \times 10^{-5}\,\text{A m}^2. \tag{13}$$

To estimate the lateral magnetic field produced by this magnetic moment, we substitute eq. (13) into eq. (12) and choose $x = h = 10$ mm which leads to $\tilde{x} = 1$. The result is

$$H_x^{(p)}(x) = 3.36\,\text{mOe} = 3.36 \times 10^{-7}\,\text{T} = 0.27\,\text{A m}^{-1}. \tag{14}$$

Now we determine the desirable values of the oscillation frequency of the magnetic dipole which depends on the plate material. Good metals, such as copper, are preferable for our purposes. The plasma frequency and the relaxation parameter of copper are equal to [57] $\omega_p = 1.12 \times 10^{16}$ rad/s and $\gamma = 1.38 \times 10^{13}$ rad/s, respectively. At low frequencies the dielectric permittivity is well described by the Drude model,

$$\varepsilon_D(\omega) = 1 - \frac{\omega_p^2}{\omega(\omega + i\gamma)}. \tag{15}$$

The oscillation frequency of the magnetic dipole has to satisfy two requirements. First, it has to provide greater reflectance on the plate. Second, it has to give large difference between the predicted field components when one uses alternative models of the dielectric response of metal.

To comply with these requirements, we introduce the quantity

$$w = hq = h\sqrt{k_t^2 - k_0^2} \tag{16}$$

and bring the reflection coefficient R_s defined in eq. (5) to the form

$$R_s(\omega, k_t) = \frac{w - \sqrt{w^2 - K(\omega)}}{w + \sqrt{w^2 - K(\omega)}}, \tag{17}$$

where

$$K(\omega) \equiv [\varepsilon(\omega) - 1]\frac{\omega^2}{\omega_h^2} \tag{18}$$

and $\omega_h = c/h$.

When the Drude model (15) is used, the major contribution to $|K(\omega)|$ at low frequencies is given by its imaginary part

$$|K(\omega)| = \frac{\omega_p^2 \gamma \omega}{(\omega^2+\gamma^2)\omega_h^2} \approx \frac{\omega_p^2 \omega}{\gamma \omega_h^2}. \tag{19}$$

With the proviso that $|K(\omega)| \gg 1$, the magnitude of the reflection coefficient (17) is close to that given by the plasma model which disregards the relaxation properties of conduction electrons,

$$\varepsilon_{pl}(\omega) = 1 - \frac{\omega_p^2}{\omega^2}. \tag{20}$$

As discussed in the introduction, the Lifshitz theory of Casimir force is in agreement with the measurement data of high-precision experiments when the plasma model is used as a response function of metals to the low-frequency s-polarized evanescent waves.

If, on the contrary, $|K(\omega)| \ll 1$, the magnitude of the reflection coefficient (17) becomes too small and only a small share of the dipole field is reflected from the plate. Because of this the dipole oscillation frequency should satisfy the condition

$$|K(\omega)| \approx \frac{\omega_p^2 \omega}{\gamma \omega_h^2} \leqslant 1, \qquad \omega \leqslant \Omega \equiv \frac{\gamma \omega_h^2}{\omega_p^2}. \tag{21}$$

For $h = 10$ mm and the Drude parameters of copper listed above, one finds $\Omega \approx 100$ rad/s. Based on this, it is reasonable to consider the dipole oscillation frequencies equal to 2, 10, and 100 rad/s, which lead to the measurable magnetic fields.

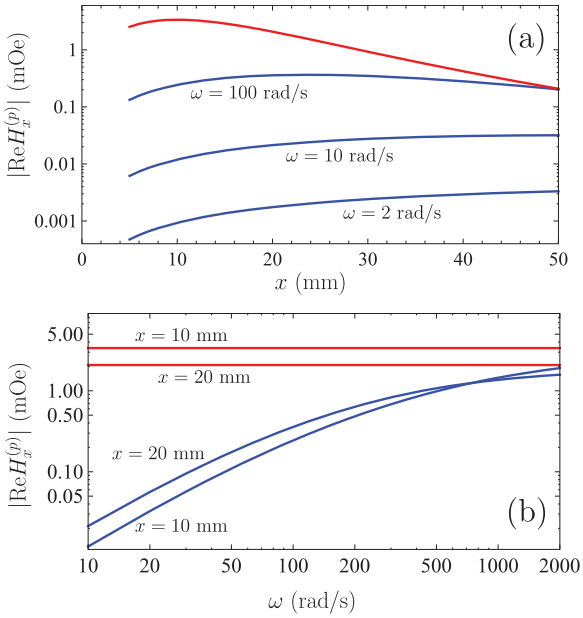

Fig. 2: The magnitude of the real part of the x-component of the magnetic field of the magnetic dipole reflected from the copper plate is shown (a) as a function of separation by the three curves counted from bottom computed using the Drude model for different dipole oscillation frequencies and by the top curve computed using the plasma model and (b) as a function of frequency by the bottom and top pairs of curves computed using the Drude and plasma models, respectively, at two different separations.

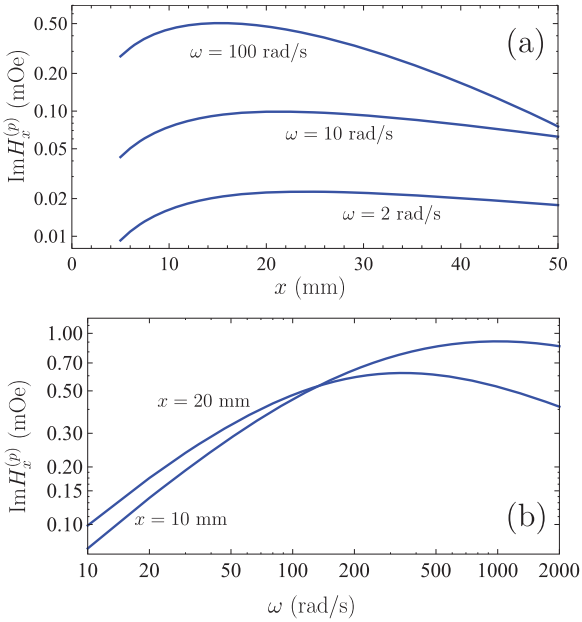

Fig. 3: The imaginary part of the x-component of magnetic field for copper plate is shown (a) as a function of separation by the three curves computed using the Drude model for different dipole oscillation frequencies and (b) as a function of frequency by two curves computed using the Drude model at two different separations. For the plasma model, the imaginary part of the field is zero.

Computational results. – We have performed numerical computations of the lateral component of the field $H_x^{(p)}$ for a magnetic dipole with the magnetic moment (13) spaced above a thick copper plate at the height of $h = 10\,\mathrm{mm}$ as shown in fig. 1. All computations were made by eq. (9) for $y = 0$, *i.e.*, $r_t = x$, using the dielectric permittivities of the Drude model (15), plasma model (20), and the spatially nonlocal phenomenological dielectric permittivity introduced [53] to reach an agreement between the Lifshitz theory and the measurement data of high-precision experiments without disregarding the relaxation properties of conduction electrons. We recall that eq. (9) describes the field component at the height h above the plate at a distance x from the magnetic dipole.

The computational results for the magnitude of the real part of $H_x^{(p)}$ are shown in fig. 2(a) as a function of the separation from the magnetic dipole. The three curves counted from the bottom are computed using the Drude model (15) for the dipole oscillation frequencies equal to 2, 10, and 100 rad/s, respectively. The top curve, which does not depend on frequency, is computed by means of the plasma model (20). In fig. 2(b), the magnitude of the real part of $H_x^{(p)}$ is shown as a function of the dipole oscillation frequency. The bottom pair of curves is computed using the Drude model at 10 and 20 mm separation from the magnetic dipole whereas the top pair of lines is computed at the same separations by means of the plasma model. In both figs. 2(a) and (b), the computational results obtained using the spatially nonlocal model [53] are indistinguishable from those shown for the plasma model.

From fig. 2 it is seen that the computational results essentially depend on whether the Drude or the plasma model is used in computations. Thus, for $|\mathrm{Re}H_x^{(p)}|$ the respective difference may be up to a factor of 10^3 depending on the dipole oscillation frequency. With increasing frequency, this difference decreases. In order to deal with not-too-small fields, we consider the oscillation frequency of 100 rad/s. In this case in the interval from 10 to 20 mm one obtains

$$|\mathrm{Re}H_x^{(p)}| \lesssim 0.336\,\mathrm{mOe} = 3.36 \times 10^{-8}\,\mathrm{T} = 0.027\,\mathrm{A\ m^{-1}} \tag{22}$$

if the Drude model is used in computations. If, however, the plasma model is used, the values of $|\mathrm{Re}H_x^{(p)}|$ at the same separations are by more than an order of magnitude larger. In doing so the parameter $k_0 r$ discussed above is of the order of 10^{-9}. This allows clear experimental discrimination between the two models of dielectric response to the low-frequency s-polarized evanescent waves (note that the current limit for the resolution of weak magnetic fields is down to $10^{-13}\,\mathrm{T}$ [58–60]).

Figure 2(b) also demonstrates a profound effect of the used dielectric model on the value of $|\mathrm{Re}H_x^{(p)}|$. Thus, the largest deviation between the theoretical predictions obtained using the Drude and plasma models by the factor

of 280 is obtained for $\omega = 10\,\mathrm{rad/s}$ at $x = 10\,\mathrm{mm}$. For $\omega = 100\,\mathrm{rad/s}$ these predictions still differ by the factor of 14.

Similar computations with all the same parameters using the Drude model have been performed for $\mathrm{Im}H_x^{(p)}$. In fig. 3(a), the obtained results are shown as a function of separation by the three curves from bottom to top for the dipole oscillation frequency equal to 2, 10, and 100 rad/s, respectively. In fig. 3(b), $\mathrm{Im}H_x^{(p)}$ is plotted as a function of frequency by the two curves computed at the separation from the dipole of 10 and 20 mm. If the plasma model is used, the reflection coefficient $R_s(\omega, k_t)$ is real resulting in $\mathrm{Im}H_x^{(p)} = 0$ (for the spatially nonlocal model [53] the values of $\mathrm{Im}H_x^{(p)}$ are by the factor of 10^{-11} smaller than those shown by the bottom line in fig. 3(a)).

From fig. 3 it is seen that if computations are performed by means of the Drude model, the obtained values of $\mathrm{Im}H_x^{(p)}$ are much greater than those of $|\mathrm{Re}H_x^{(p)}|$ shown in fig. 2 for all values of the oscillation frequency. It is evident also that any nonzero measured value of $\mathrm{Im}H_x^{(p)}$ could be used in support of the Drude model and for an exclusion of the plasma model as a response function to the low-frequency s-polarized evanescent waves.

Conclusions. – In the foregoing, it was argued that there are no sufficient experimental evidences in favor of the statement that the response of metals to the low-frequency s-polarized evanescent waves is described by the dielectric permittivity of the Drude model. Additional importance to this statement is added by the fact that the Lifshitz theory of the Casimir force becomes inconsistent with the measurement data of a number of high-precision experiments if the electromagnetic response of metals at low frequencies is described by the Drude model. An agreement between the experiment and theory is restored if, instead, the plasma model is used. Thus, a direct experimental test of the response function of metals to the s-polarized evanescent waves is crucial for both the Casimir effect and for all numerous applications of these waves in fundamental physics and in modern technology.

According to the obtained results, the direct experimental test for the Drude dielectric permittivity as a response function of metals to the low-frequency s-polarized evanescent waves can be performed by measuring the lateral component of the magnetic field of the oscillating magnetic dipole spaced above a thick metallic plate. To prove this statement, we have derived an analytic expression for the magnetic field of a small magnetic dipole located in the vicinity of a metallic surface and demonstrated that its lateral component is determined by the contribution of the s-polarized evanescent waves alone. Numerical computations of the real and imaginary parts of the lateral field component were performed for a copper plate for the reasonable experimental parameters by describing the electromagnetic response of metals by the Drude or plasma models for different oscillation frequencies of the dipole. It was shown that the obtained results differ by the orders of magnitude depending on the model of dielectric permittivity used. Thus, by measuring the field components, whose values are well within the limits of experimental sensitivity, one could either validate or disprove the possibility to use the Drude model in the range of low-frequency s-polarized evanescent waves.

The results of the proposed experiment would be elucidating for the long-standing problems of the Lifshitz theory and will find applications in the fluorescence microscopy, infrared spectroscopy, theory of superlenses, surface plasmon polaritons and other prospective subjects of optics and condensed matter physics.

* * *

GLK and VMM were partially supported by the Peter the Great Saint Petersburg Polytechnic University in the framework of the Russian state assignment for basic research (Project No. FSEG-2020-0024). The work of VMM was also supported by the Kazan Federal University Strategic Academic Leadership Program. VBS was partially supported by the Russian Science Foundation, grant No. 20-19-00214.

Data availability statement: The data that support the findings of this study are included within the article (and any supplementary file).

REFERENCES

[1] de Fornel F., *Evanescent Waves. From Newtonian Optics to Atomic Optics* (Springer, Berlin) 2001.
[2] Bertolotti M., Sibilia C. and Guzman A. M., *Evanescent Waves in Optics. An Introduction to Plasmonics* (Springer, Cham) 2017.
[3] Greffet J.-J. and Carminati R., *Prog. Surf. Sci.*, **56** (1997) 133.
[4] Törmä P. and Barnes W. L., *Rep. Prog. Phys.*, **78** (2015) 013901.
[5] Culshaw W. and Jones D. S., *Proc. Phys. Soc. B*, **66** (1953) 859.
[6] Brady J. J., Brick R. O. and Pearson V. D., *J. Opt. Soc. Am.*, **50** (1960) 1080.
[7] Zhu S., Yu A. W., Hawley D. and Roy R., *Am. J. Phys.*, **54** (1986) 601.
[8] Hsu J. W. P., *Mater. Sci. Eng. R: Rep.*, **33** (2001) 1.
[9] Aigouy L., Lahrech A., Grésillon S., Cory H., Boccara A. C. and Rivoal J. C., *Opt. Lett.*, **24** (1999) 187.
[10] Decca R. S., Fischbach E., Klimchitskaya G. L., Krause D. E., López D. and Mostepanenko V. M., *Phys. Rev. D*, **68** (2003) 116003.
[11] Decca R. S., López D., Fischbach E., Klimchitskaya G. L., Krause D. E. and Mostepanenko V. M., *Ann. Phys. (N.Y.)*, **318** (2005) 37.
[12] Decca R. S., López D., Fischbach E., Klimchitskaya G. L., Krause D. E. and Mostepanenko V. M., *Phys. Rev. D*, **75** (2007) 077101.

[13] Decca R. S., López D., Fischbach E., Klimchitskaya G. L., Krause D. E. and Mostepanenko V. M., *Eur. Phys. J. C*, **51** (2007) 963.

[14] Bimonte G., López D. and Decca R. S., *Phys. Rev. B*, **93** (2016) 184434.

[15] Bimonte G., Spreng B., Maia Neto P. A., Ingold G.-L., Klimchitskaya G. L., Mostepanenko V. M. and Decca R. S., *Universe*, **7** (2021) 93.

[16] Chang C.-C., Banishev A. A., Castillo-Garza R., Klimchitskaya G. L., Mostepanenko V. M. and Mohideen U., *Phys. Rev. B*, **85** (2012) 165443.

[17] Banishev A. A., Chang C.-C., Klimchitskaya G. L., Mostepanenko V. M. and Mohideen U., *Phys. Rev. B*, **85** (2012) 195422.

[18] Banishev A. A., Klimchitskaya G. L., Mostepanenko V. M. and Mohideen U., *Phys. Rev. Lett.*, **110** (2013) 137401.

[19] Banishev A. A., Klimchitskaya G. L., Mostepanenko V. M. and Mohideen U., *Phys. Rev. B*, **88** (2013) 155410.

[20] Xu J., Klimchitskaya G. L., Mostepanenko V. M. and Mohideen U., *Phys. Rev. A*, **97** (2018) 032501.

[21] Liu M., Xu J., Klimchitskaya G. L., Mostepanenko V. M. and Mohideen U., *Phys. Rev. B*, **100** (2019) 081406(R).

[22] Liu M., Xu J., Klimchitskaya G. L., Mostepanenko V. M. and Mohideen U., *Phys. Rev. A*, **100** (2019) 052511.

[23] Lifshitz E. M., *Zh. Eksp. Teor. Fiz.*, **29** (1955) 94; *Sov. Phys. JETP*, **2** (1956) 73.

[24] Dzyaloshinskii I. E., Lifshitz E. M. and Pitaevskii L. P., *Usp. Fiz. Nauk*, **73** (1961) 381; *Adv. Phys.*, **10** (1961) 165.

[25] Lifshitz E. M. and Pitaevskii L. P., *Statistical Physics, Part II* (Pergamon, Oxford) 1980.

[26] Henkel C., Joulain K., Mulet J.-Ph. and Greffet J.-J., *Phys. Rev. A*, **69** (2004) 023808.

[27] Torgerson J. R. and Lamoreaux S. K., *Phys. Rev. E*, **70** (2004) 047102.

[28] Intravaia F. and Lambrecht A., *Phys. Rev. Lett.*, **94** (2005) 110404.

[29] Bimonte G., *Phys. Rev. E*, **73** (2006) 048101.

[30] Bordag M., *J. Phys. A: Math. Gen.*, **39** (2006) 6173.

[31] Svetovoy V. B. and Esquivel R., *J. Phys. A: Math. Gen.*, **39** (2006) 6777.

[32] Klimchitskaya G. L., Mohideen U. and Mostepanenko V. M., *Rev. Mod. Phys.*, **81** (2009) 1827.

[33] Bordag M., Klimchitskaya G. L., Mohideen U. and Mostepanenko V. M., *Advances in the Casimir Effect* (Oxford University Press, Oxford) 2015.

[34] Woods L. M., Dalvit D. A. R., Tkatchenko A., Rodriguez-Lopez P., Rodriguez A. W. and Podgornik R., *Rev. Mod. Phys.*, **88** (2016) 045003.

[35] Landau L. D. and Lifshitz E. M., *The Classical Theory of Fields* (Pergamon, Oxford) 1971.

[36] Abramowitz M. and Stegun I. A. (Editors), *Handbook of Mathematical Functions With Formulas, Graphs, and Mathematical Tables* (National Bureau of Standards, Washington) 1964.

[37] Prudnikov A. P., Brychkov Yu. A. and Marichev O. I., *Integrals and Series*, Vol. **1**: *Elementary Functions* (Gordon and Breach, New York) (1986).

[38] Prudnikov A. P., Brychkov Yu. A. and Marichev O. I., *Integrals and Series*, Vol. **2**: *Special Functions* (Gordon and Breach, New York) (1986).

[39] Reitz J. R., *J. Appl. Phys.*, **41** (1970) 2067.

[40] Saslow W. M., *Am. J. Phys.*, **60** (1992) 693.

[41] Skaar J., *Eur. J. Phys.*, **40** (2019) 045201.

[42] Kats E. I., *Zh. Eksp. Teor. Fiz.*, **73** (1977) 212; *Sov. Phys. JETP*, **46** (1977) 109.

[43] Svetovoy V. B. and Lokhanin M. V., *Phys. Rev. A*, **67** (2003) 022113.

[44] Esquivel R., Villarreal C. and Mochán W. L., *Phys. Rev. A*, **68** (2003) 052103; **71** (2005) 029904(E).

[45] Esquivel R. and Svetovoy V. B., *Phys. Rev. A*, **69** (2004) 062102.

[46] Svetovoy V. B. and Esquivel R., *Phys. Rev. E*, **72** (2005) 036113.

[47] Sernelius Bo E., *Phys. Rev. B*, **71** (2005) 235114.

[48] Haakh H. R. and Henkel C., *Eur. Phys. J. B*, **85** (2012) 46.

[49] Klimchitskaya G. L. and Mostepanenko V. M., *Eur. Phys. J. C*, **80** (2020) 900.

[50] Klimchitskaya G. L. and Mostepanenko V. M., *Phys. Rev. D*, **104** (2021) 085001.

[51] Klimchitskaya G. L. and Mostepanenko V. M., *Phys. Rev. D*, **103** (2021) 096007.

[52] Hannemann M., Wegner G. and Henkel C., *Universe*, **7** (2021) 108.

[53] Klimchitskaya G. L. and Mostepanenko V. M., *Phys. Rev. A*, **105** (2022) 012805.

[54] Drndić M., Johnson K. S., Thywissen J. H., Prentiss M. and Westervelt R. M., *Appl. Phys. Lett.*, **72** (1998) 2906.

[55] Ramadan Q., Samper V., Poenar D. and Yu C., *J. Magn. & Magn. Mater.*, **281** (2004) 150.

[56] Wensink H., Benito-Lopez F., Hermes D. C., Verboom W., Gardeniers H. J. G. E., Reinhoudt D. N. and van den Berg A., *Lab Chip*, **5** (2005) 280.

[57] Ordal M. A., Bell R. J., Alexander R. W., Long L. L. and Querry M. R., *Appl. Opt.*, **24** (1985) 4493.

[58] Liu Zeng-Xing, Wang Bao, Kong Cui, Si Liu-Gang, Xiong Hao and Wu Ying, *Sci. Rep.*, **7** (2017) 12521.

[59] Murzin D., Mapps D. J., Levada K., Belyaev V., Omelyanchik A., Panina L. and Rodionova V., *Sensors*, **20** (2020) 1569.

[60] Huang Jing-Hui, Duan Xue-Ying, Wang Guang-Jun and Hu Xiang-Yun, *J. Opt. Soc. Am. B*, **39** (2022) 1289.